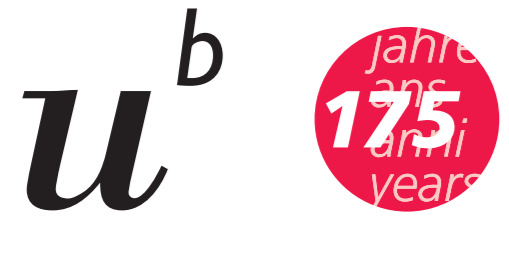


Quality-Guided Synchrotron-based Tomographic Microscopy of Large Lung Samples



UNIVERSITÄT
BERN



David Haberthür¹, Christoph Hintermüller², Federica Marone²,
Johannes Schittny¹ and Marco Stampanoni^{2,3}

¹Institute of Anatomy, University of Bern, Switzerland, ²Swiss Light Source, Paul Scherrer Institut, Villigen, Switzerland, ³Institute of Biomedical Engineering, University and ETH Zürich, Switzerland
haberthuer@ana.unibe.ch, marco.stampanoni@psi.ch

INTRODUCTION

THE acinus represents the functional lung unit of the pulmonary gas-exchange area. Until now, the investigation of full acini was either limited by the resolution of the imaging method or the sample volume. Even if synchrotron-based tomographic microscopy (SRXTM) can be used at a resolution down to a voxel size of 360 nm, the available sample volume at this resolution was limited. At the TOMCAT beamline [1] at the Swiss Light Source of the Paul Scherrer Institut in Villigen, Switzerland we developed a method to combine multiple, independently acquired synchrotron-based x-ray tomographic scans to one large three-dimensional object.

THE field of view of tomographic scans can be increased through stacking of several acquired tomograms parallel to the beam (figure 1(a)). To increase the field of view in perpendicular direction, the acquired projection images of the sample have to be merged into one large projection image prior to reconstructing the sample (figure 1(b)).

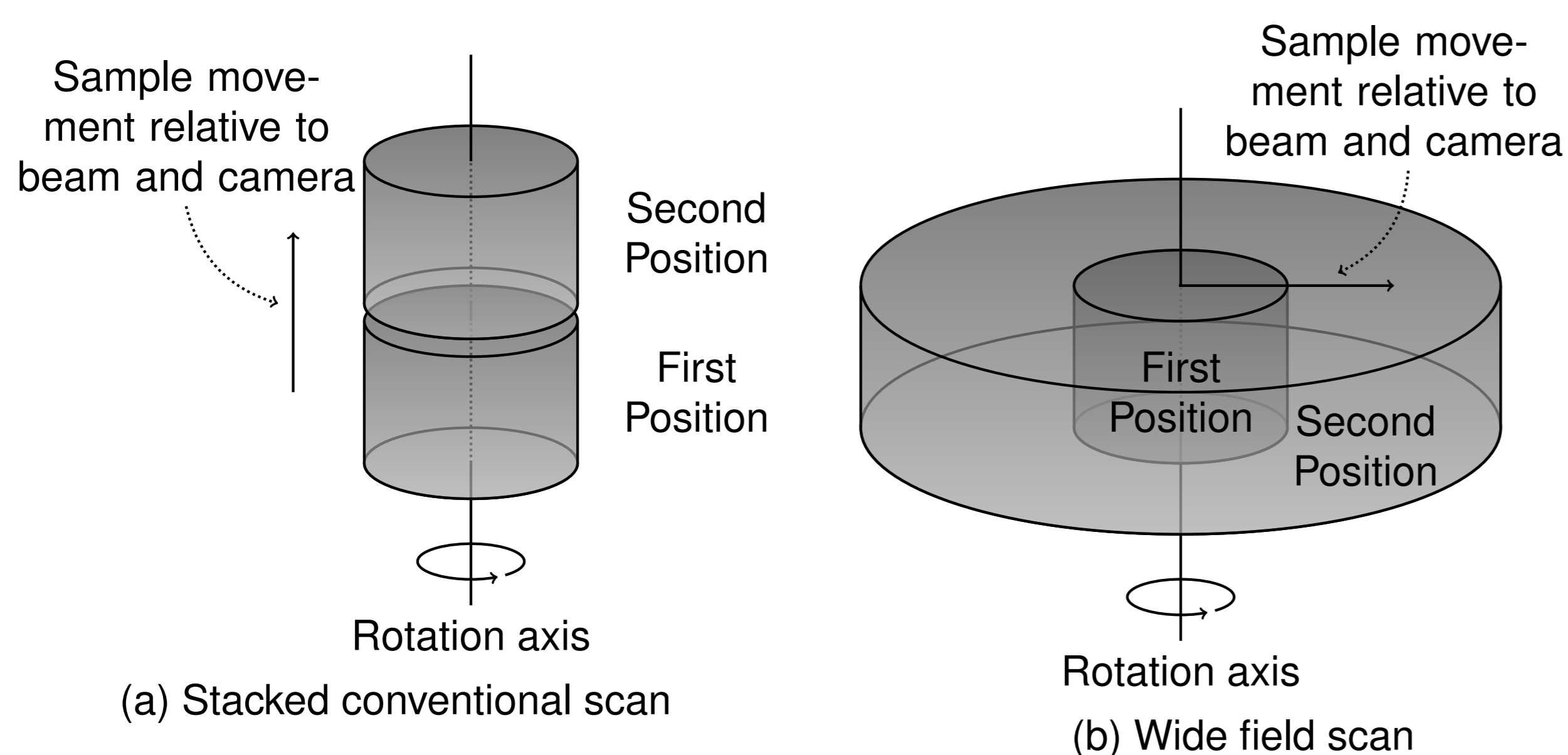


Figure 1: Enhancing the field of view of tomography based imaging methods: Top: Stacking several scans in parallel direction. Bottom: Merging several scans in perpendicular direction.

MATERIALS AND METHODS

TO fulfill the sampling theorem, an increased amount of projections has to be acquired for the lateral parts of the sample. Merging scans laterally increases the total scanning time, since the time needed to acquire a scan scales linearly with the amount of recorded projections. Different scanning protocols have been defined, varying in the total amount of projections recorded for each subscan position.

A sequence of 19 such protocols of the same sample—a distal-medial edge of the right lower lung lobe of a Sprague Dawley rat, obtained postnatally at day 21 [2]—has been scanned to verify the predictions made from the simulations of the expected image quality.

RESULTS

THE quality of each of the 19 protocols (B–T) was simulated using a Shepp–Logan phantom and compared to a gold standard simulation (red dots in figure 2). The experimentally derived scan quality was computed as the difference between the reconstructed slices of each of the 19 protocols (blue diamonds in figure 2) and the scanned gold standard protocol (marked as B).

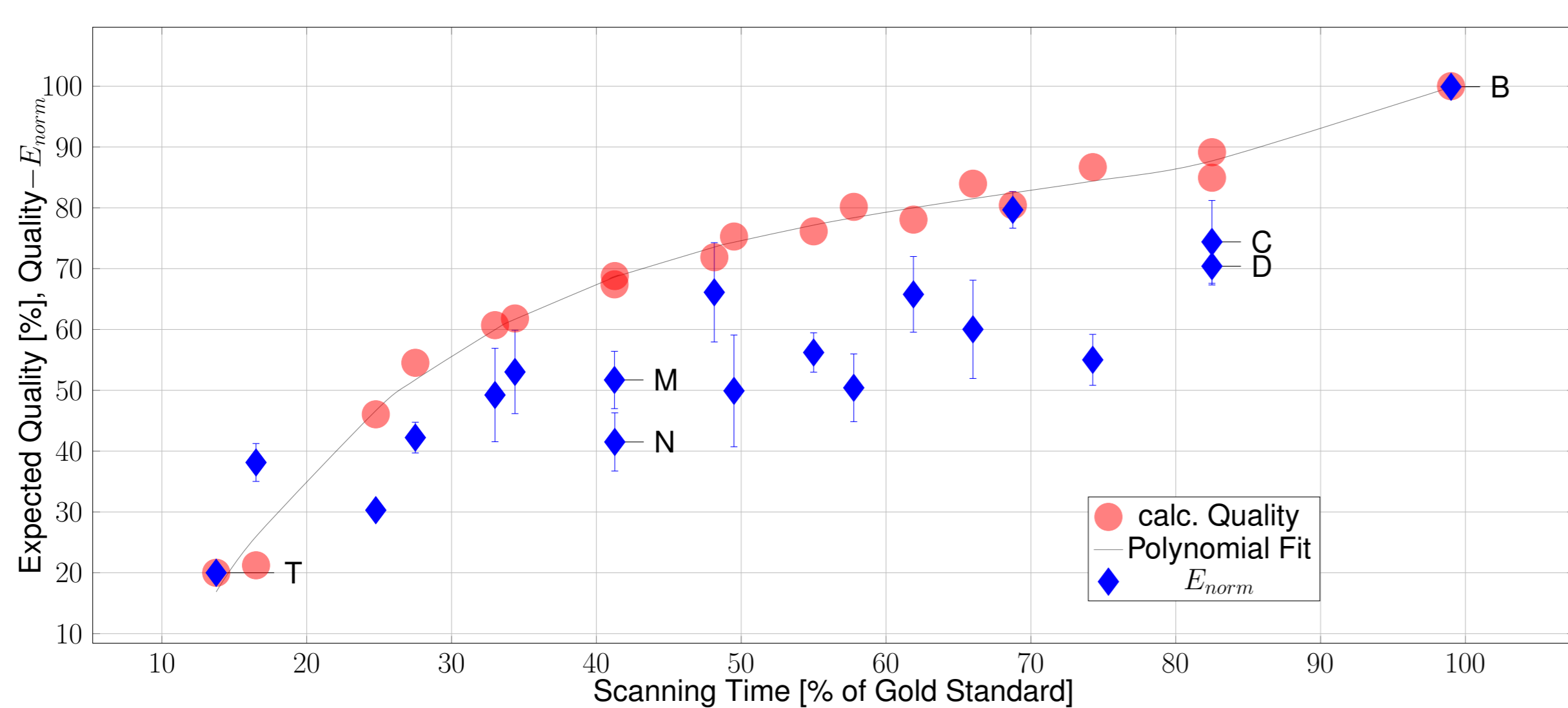


Figure 2: Plot of normalized difference Value (E_{norm} , blue diamonds) for the 19 scanned protocols overlaid over Quality-plot obtained from the simulation (red dots). The error bars for each protocol show the standard deviation of the error calculated for 205 of the 1024 slices for each of the 19 protocols. The abscissa shows the scanning time in percentage of time used for the gold standard scan.

WE were able to decrease the scanning time by 86% while keeping the quality of the tomographic datasets at a level which permits automatic segmentation and three-dimensional visualization. The three-dimensional reconstructions in figure 3 show two examples of the 19 scanned protocols and show a three-fold increase in the field of view. A difference between reconstructions of airway segments is only visible in high magnification (figures 3(c) and (d)).

FURTHER increasing the field of view is possible by acquiring additional lateral scans. A sample scanned with a five-fold increased field of view is shown in figure 4. Additionally, multiple wide field scans can be stacked on top of each other as shown in figure 1(a).

RESULTS (CONT.)

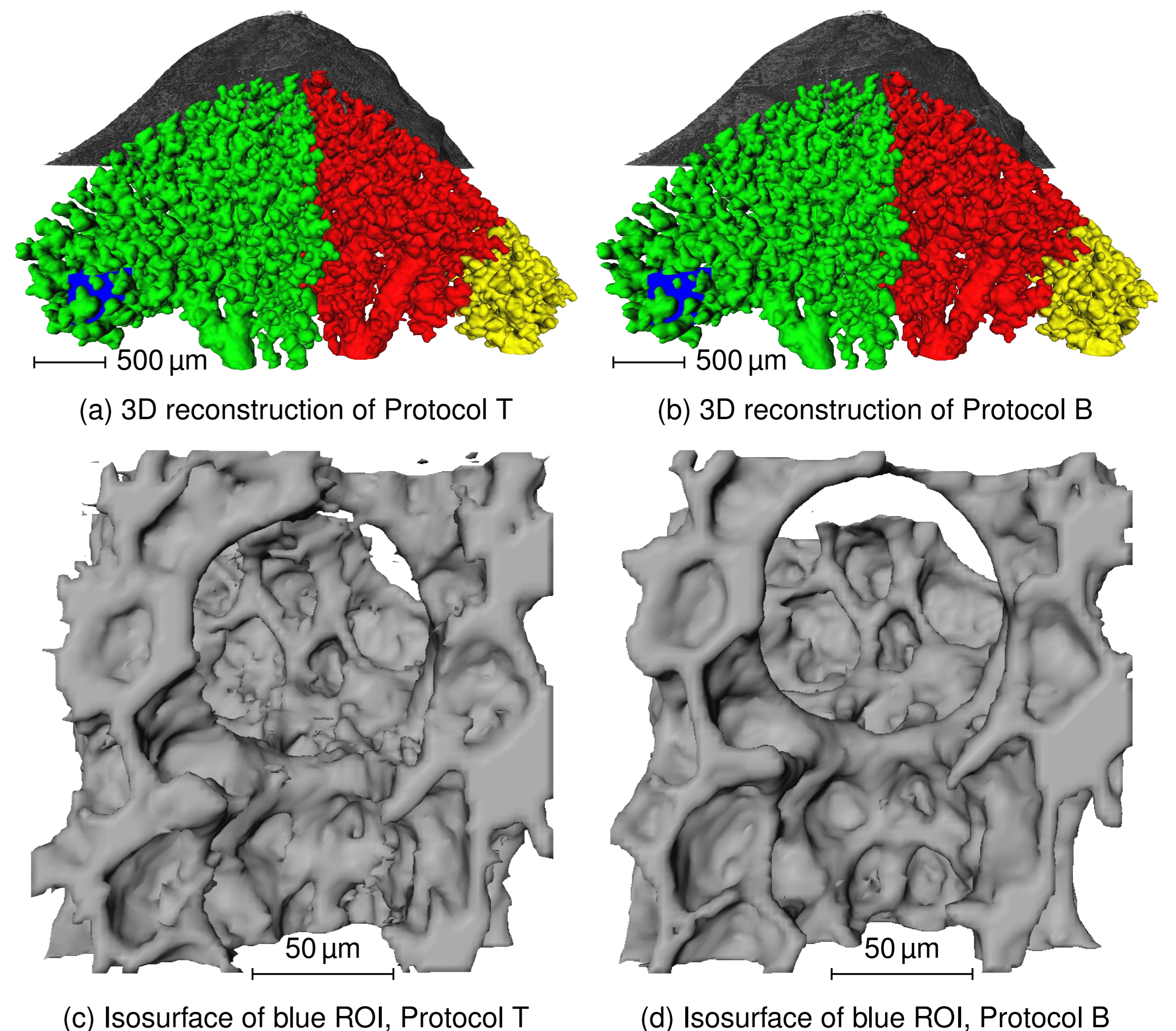


Figure 3: Three-dimensional reconstructions of the fastest (T) and the slowest (gold standard, B) protocols. a) and b): Isosurface visualizations of three independent airway segments. c) and d): Close-up view of isosurface visualizations of the blue regions of interest in the upper panels. The total acquisition time of protocol T is only 14% of the acquisition time of protocol B (9 minutes compared to 63 minutes).

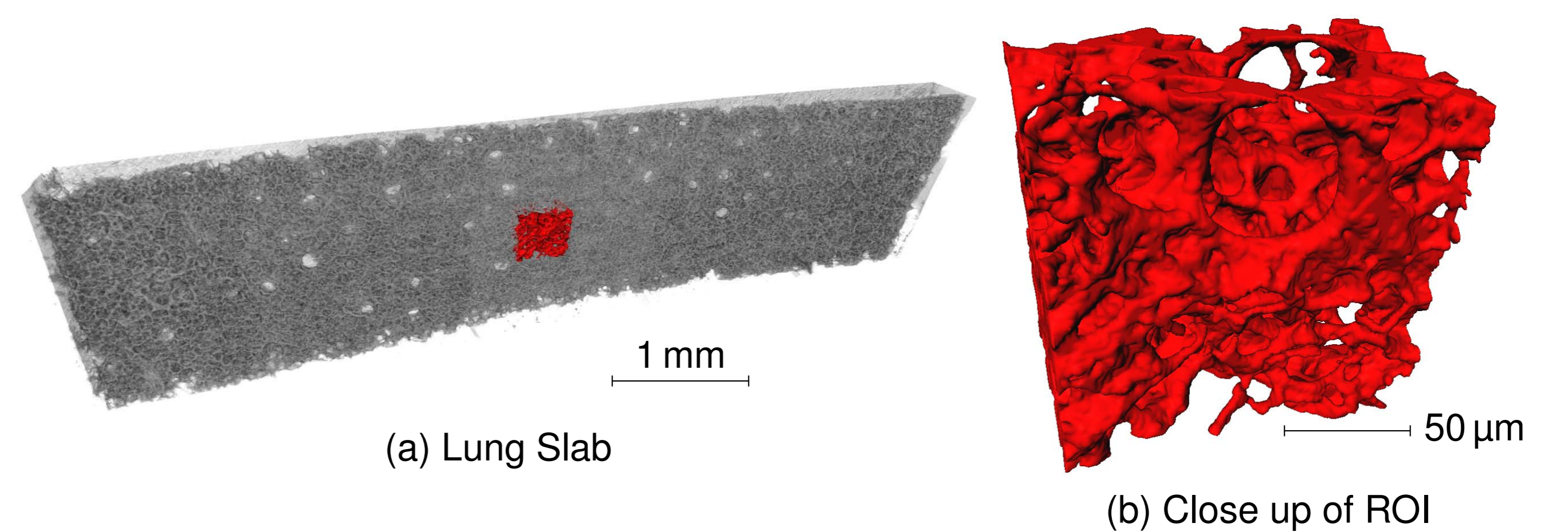


Figure 4: Visualization of lung tissue slice [3]: a): Volume rendering of slice of lung tissue with a size of $554 \times 4854 \times 1024$ pixels at a voxel size of $1.43 \mu\text{m}$. The inset red cube has a size of 128 pixels and was automatically segmented using a region growing algorithm. b): Close-up of inset cube. Single alveoli of the lung are clearly visible.

BY combining 3–5 tomographic scans perpendicular to the rotational axis, the sample volume contained in the resulting tomographic datasets could be enlarged to a cylinder of 1.5 mm in height and up to a diameter of 6.9 mm at an isometric voxel length of $1.43 \mu\text{m}$. Compared to a conventional scan, this corresponds to a nine- to 25-fold increase in visible volume.

DISCUSSION

THE proposed method increases the lateral field of view of TOMCAT while providing a method of objectively choosing a scanning protocol based on scanning time and reconstruction quality. Wide field SRXTM enables us to acquire tomographic datasets of large sample volumes at high resolution. In advantage to classic SRXTM we are now able to obtain unrestricted high resolution three-dimensional views of single acini, the structural units of the lung (see also Poster I-8).

ACKNOWLEDGMENTS

THIS work has been funded by grant #3100A0-109874 of the Swiss National Science Foundation. We thank Mohammed Ouanella for expert help with the preparation of the samples and Dipl.-Ing. Sophie Rausch of the Institute for Computational Mechanics, Technische Universität München for providing the lung samples shown in figure 4.

References

- [1] M. Stampanoni, A. Groso, A. Isenegger, G. Mikuljan, Q. Chen, D. Meister, M. Lange, R. Betemps, S. Henein, and R. Abela. TOMCAT: A beamline for Tomographic Microscopy and Coherent Radiology experiments. *AIP Conference Proceedings*, 879(1):848–851, 2007. doi: 10.1063/1.2436193.
- [2] Johannes C. Schittny, Sonja I. Mund, and Marco Stampanoni. Evidence and structural mechanism for late lung alveolarization. *Am J Physiol Lung Cell Mol Physiol*, 294(2):L246–254, 2008. doi: 10.1152/ajplung.00296.2007.
- [3] S. Rausch, C. Dassow, S. Uhlig, and W. A. Wall. Determination of Material Parameters of Lung Parenchyma Based on Living Precision-Cut Lung Slices Testing. *Journal for Biomechanical Engineering*, 2009. in preparation.